The Astrophysical Journal Letters, 961:L8 (12pp), 2024 January 20 https://doi.org/10.3847/2041-8213/ad1832

X-Ray Polarized View of the Accretion Geometry in the X-Ray Binary Circinus X-1

John Rankin[1], Fabio La Monaca[1,2,3], Alessandro Di Marco[1], Juri Poutanen[4], Anna Bobrikova[4], Vadim Kravtsov[4], Fabio Muleri[1], Maura Pilia[5], Alexandra Veledina[4,6], Rob Fender[7], Philip Kaaret[8], Dawoon E. Kim[1,2,3], Andrea Marinucci[9], Herman L. Marshall[10], Alessandro Papitto[11], Allyn F. Tennant[8], Sergey S. Tsygankov[4], Martin C. Weisskopf[8], Kinwah Wu[12], Silvia Zane[12], Filippo Ambrosino[11], Ruben Farinelli[13], Andrea Gnarini[14], Iván Agudo[15], Lucio A. Antonelli[11,16], Matteo Bachetti[5], Luca Baldini[17,18], Wayne H. Baumgartner[8], Ronaldo Bellazzini[17], Stefano Bianchi[14], Stephen D. Bongiorno[8], Raffaella Bonino[19,20], Alessandro Brez[17], Niccolò Bucciantini[21,22,23], Fiamma Capitanio[1], Simone Castellano[17], Elisabetta Cavazzuti[9], Chien-Ting Chen[24], Stefano Ciprini[16,25], Enrico Costa[1], Alessandra De Rosa[1], Ettore Del Monte[1], Laura Di Gesu[9], Niccolò Di Lalla[26], Immacolata Donnarumma[9], Victor Doroshenko[27], Michal Dovčiak[28], Steven R. Ehlert[8], Teruaki Enoto[29], Yuri Evangelista[1], Sergio Fabiani[1], Riccardo Ferrazzoli[1], Javier A. Garcia[30], Shuichi Gunji[31], Kiyoshi Hayashida[32,53], Jeremy Heyl[33], Wataru Iwakiri[34], Svetlana G. Jorstad[35,36], Vladimir Karas[28], Fabian Kislat[37], Takao Kitaguchi[29], Jeffery J. Kolodziejczak[8], Henric Krawczynski[38], Luca Latronico[19], Ioannis Liodakis[8], Simone Maldera[19], Alberto Manfreda[39], Frédéric Marin[40], Alan P. Marscher[35], Francesco Massaro[19,20], Giorgio Matt[14], Ikuyuki Mitsuishi[41], Tsunefumi Mizuno[42], Michela Negro[43], Chi-Yung Ng[44], Stephen L. O'Dell[8], Nicola Omodei[26], Chiara Oppedisano[19], George G. Pavlov[45], Abel L. Peirson[26], Matteo Perri[11,16], Melissa Pesce-Rollins[17], Pierre-Olivier Petrucci[46], Andrea Possenti[5], Simonetta Puccetti[16], Brian D. Ramsey[8], Ajay Ratheesh[1], Oliver J. Roberts[24], Roger W. Romani[26], Carmelo Sgrò[17], Patrick Slane[47], Paolo Soffitta[1], Gloria Spandre[17], Douglas A. Swartz[24], Toru Tamagawa[29], Fabrizio Tavecchio[48], Roberto Taverna[49], Yuzuru Tawara[41], Nicholas E. Thomas[8], Francesco Tombesi[2,25,50], Alessio Trois[5], Roberto Turolla[12,49], Jacco Vink[51], and Fei Xie[1,52]

[1] INAF Istituto di Astrofisica e Planetologia Spaziali, Via del Fosso del Cavaliere 100, I-00133 Roma, Italy
[2] Dipartimento di Fisica, Università degli Studi di Roma "Tor Vergata," Via della Ricerca Scientifica 1, I-00133 Roma, Italy
[3] Dipartimento di Fisica, Università degli Studi di Roma "La Sapienza," Piazzale Aldo Moro 5, I-00185 Roma, Italy
[4] Department of Physics and Astronomy, 20014 University of Turku, Finland
[5] INAF Osservatorio Astronomico di Cagliari, Via della Scienza 5, I-09047 Selargius (CA), Italy
[6] Nordita, KTH Royal Institute of Technology and Stockholm University, Hannes Alfvéns väg 12, SE-106 91, Sweden
[7] Department of Physics, University of Oxford, Denys Wilkinson Building, Keble Road, Oxford OX1 3RH, UK
[8] NASA Marshall Space Flight Center, Huntsville, AL 35812, USA
[9] Agenzia Spaziale Italiana, Via del Politecnico snc, I-00133 Roma, Italy
[10] MIT Kavli Institute for Astrophysics and Space Research, Massachusetts Institute of Technology, 77 Massachusetts Avenue, Cambridge, MA 02139, USA
[11] INAF Osservatorio Astronomico di Roma, Via Frascati 33, I-00040 Monte Porzio Catone (RM), Italy
[12] Mullard Space Science Laboratory, University College London, Holmbury St Mary, Dorking, Surrey RH5 6NT, UK
[13] INAF Osservatorio di Astrofisica e Scienza dello Spazio di Bologna, Via P. Gobetti 101, I-40129 Bologna, Italy
[14] Dipartimento di Matematica e Fisica, Università degli Studi Roma Tre, Via della Vasca Navale 84, I-00146 Roma, Italy
[15] Instituto de Astrofísica de Andalucía—CSIC, Glorieta de la Astronomía s/n, E-18008 Granada, Spain
[16] Space Science Data Center, Agenzia Spaziale Italiana, Via del Politecnico snc, I-00133 Roma, Italy
[17] Istituto Nazionale di Fisica Nucleare, Sezione di Pisa, Largo B. Pontecorvo 3, I-56127 Pisa, Italy
[18] Dipartimento di Fisica, Università di Pisa, Largo B. Pontecorvo 3, I-56127 Pisa, Italy
[19] Istituto Nazionale di Fisica Nucleare, Sezione di Torino, Via Pietro Giuria 1, I-10125 Torino, Italy
[20] Dipartimento di Fisica, Università degli Studi di Torino, Via Pietro Giuria 1, I-10125 Torino, Italy
[21] INAF Osservatorio Astrofisico di Arcetri, Largo Enrico Fermi 5, I-50125 Firenze, Italy
[22] Dipartimento di Fisica e Astronomia, Università degli Studi di Firenze, Via Sansone 1, I-50019 Sesto Fiorentino (FI), Italy
[23] Istituto Nazionale di Fisica Nucleare, Sezione di Firenze, Via Sansone 1, I-50019 Sesto Fiorentino (FI), Italy
[24] Science and Technology Institute, Universities Space Research Association, Huntsville, AL 35805, USA
[25] Istituto Nazionale di Fisica Nucleare, Sezione di Roma "Tor Vergata," Via della Ricerca Scientifica 1, I-00133 Roma, Italy
[26] Department of Physics and Kavli Institute for Particle Astrophysics and Cosmology, Stanford University, Stanford, CA 94305, USA
[27] Institut für Astronomie und Astrophysik, Universität Tübingen, Sand 1, D-72076 Tübingen, Germany
[28] Astronomical Institute of the Czech Academy of Sciences, Boční II 1401/1, 14100 Praha 4, Czech Republic
[29] RIKEN Cluster for Pioneering Research, 2-1 Hirosawa, Wako, Saitama 351-0198, Japan
[30] NASA Goddard Space Flight Center, Greenbelt, MD 20771, USA
[31] Yamagata University,1-4-12 Kojirakawa-machi, Yamagata-shi 990-8560, Japan
[32] Osaka University, 1-1 Yamadaoka, Suita, Osaka 565-0871, Japan
[33] University of British Columbia, Vancouver, BC V6T 1Z4, Canada
[34] International Center for Hadron Astrophysics, Chiba University, Chiba 263-8522, Japan
[35] Institute for Astrophysical Research, Boston University, 725 Commonwealth Avenue, Boston, MA 02215, USA
[36] Department of Astrophysics, St. Petersburg State University, Universitetsky pr. 28, Petrodvoretz, 198504 St. Petersburg, Russia
[37] Department of Physics and Astronomy and Space Science Center, University of New Hampshire, Durham, NH 03824, USA
[38] Physics Department and McDonnell Center for the Space Sciences, Washington University in St. Louis, St. Louis, MO 63130, USA
[39] Istituto Nazionale di Fisica Nucleare, Sezione di Napoli, Strada Comunale Cinthia, I-80126 Napoli, Italy
[40] Université de Strasbourg, CNRS, Observatoire Astronomique de Strasbourg, UMR 7550, F-67000 Strasbourg, France
[41] Graduate School of Science, Division of Particle and Astrophysical Science, Nagoya University, Furo-cho, Chikusa-ku, Nagoya, Aichi 464-8602, Japan
[42] Hiroshima Astrophysical Science Center, Hiroshima University, 1-3-1 Kagamiyama, Higashi-Hiroshima, Hiroshima 739-8526, Japan
[43] Department of Physics and Astronomy, Louisiana State University, Baton Rouge, LA 70803, USA
[44] Department of Physics, University of Hong Kong, Pokfulam, Hong Kong
[45] Department of Astronomy and Astrophysics, Pennsylvania State University, University Park, PA 16801, USA
[46] Université Grenoble Alpes, CNRS, IPAG, F-38000 Grenoble, France

[47] Center for Astrophysics, Harvard & Smithsonian, 60 Garden Street, Cambridge, MA 02138, USA
[48] INAF Osservatorio Astronomico di Brera, via E. Bianchi 46, I-23807 Merate (LC), Italy
[49] Dipartimento di Fisica e Astronomia, Università degli Studi di Padova, Via Marzolo 8, I-35131 Padova, Italy
[50] Department of Astronomy, University of Maryland, College Park, MD 20742, USA
[51] Anton Pannekoek Institute for Astronomy & GRAPPA, University of Amsterdam, Science Park 904, 1098 XH Amsterdam, The Netherlands
[52] Guangxi Key Laboratory for Relativistic Astrophysics, School of Physical Science and Technology, Guangxi University, Nanning 530004, People's Republic of China
Received 2023 November 8; revised 2023 December 21; accepted 2023 December 22; published 2024 January 11

Abstract

Cir X-1 is a neutron star X-ray binary characterized by strong variations in flux during its eccentric ∼16.6 day orbit. There are also strong variations in the spectral state, and it has historically shown both atoll and Z state properties. We observed the source with the Imaging X-ray Polarimetry Explorer during two orbital segments, 6 days apart, for a total of 263 ks. We find an X-ray polarization degree in these segments of $1.6\% \pm 0.3\%$ and $1.4\% \pm 0.3\%$ at polarization angles of $37° \pm 5°$ and $-12° \pm 7°$, respectively. Thus, we observed a rotation of the polarization angle by $49° \pm 8°$ along the orbit. Because variations of accretion flow, and then of the hardness ratio, are expected during the orbit, we also studied the polarization binned in hardness ratio and found the polarization angle differing by $67° \pm 11°$ between the lowest and highest values of the hardness ratio. We discuss possible interpretations of this result that could indicate a possible misalignment between the symmetry axes of the accretion disk and the Comptonizing region caused by the misalignment of the neutron star's angular momentum with respect to the orbital one.

Unified Astronomy Thesaurus concepts: X-ray binary stars (1811); Polarimetry (1278); X-ray astronomy (1810); X-ray sources (1822)

1. Introduction

X-ray binaries (XRBs) consist of a compact object with a stellar companion orbiting it, from which it accretes matter. Flux and spectral variations in XRBs are thought to correspond to different accretion configurations. The spectrum of each state can be interpreted as a superposition of different components having a different relative flux: typically the accretion disk, emitting a soft, nearly thermal spectrum described by a blackbody or a multicolor disk, and a corona of hot plasma, whose electrons up-scatter the low-energy ambient photons, generating a hard X-ray component. In neutron star (NS) XRBs (NS-XRBs), the surface region, where the accreting matter is stopped, also contributes to the total emission. The interfacing region, which is coplanar to the accretion disk, is known as the boundary layer (BL; Shakura & Sunyaev 1988; Popham & Sunyaev 2001), while the gas layer at the NS surface, extending up to high latitudes, is known as the spreading layer (SL; Inogamov & Sunyaev 1999; Suleimanov & Poutanen 2006; Abolmasov et al. 2020). XRBs with a weakly magnetized NS are classified, according to their tracks on the hard/soft X-ray color diagram, as Z or atoll sources (Hasinger & van der Klis 1989; van der Klis 1989).

Cir X-1 is a weakly magnetized NS-XRB characterized by an eccentric ($e \sim 0.45$) ∼16.5 day orbit (see, e.g., Kaluzienski et al. 1976; Schulz et al. 2020), during which its flux and spectrum change significantly, very different from any other known XRB. Cir X-1 has historically been shown to go through all the different states for both Z and atoll sources (Schulz et al. 2019). On the basis of its spectral characteristics, it was for a long time suspected to host a black hole, but the discovery of type I bursts undoubtedly proved that the compact object is an NS (Tennant et al. 1986; Linares et al. 2010). During its orbit, the X-ray flux varies by 2 orders of magnitude, and there are also more irregular decades-long variations (D'Aì et al. 2012).

An extended emission from a supernova remnant has been found around Cir X-1 (Heinz et al. 2013) with an estimated age of 4600 yr, implying that the source is the youngest known XRB (as reported by Heinz et al. 2013). The young age is consistent both with the eccentricity of the orbit and with its irregular variations. Another characteristic that sets Cir X-1 apart from other XRBs is the presence of both radio and—a unique case identified so far for NS-XRBs—X-ray jets, indicating the ejection of matter at relativistic speeds. The X-ray jets are clearly visible on both sides of the receding and approaching radio jet (Heinz et al. 2007; Soleri et al. 2009). Their presence, observed by Chandra either as a Doppler shift of emission lines or by directly imaging a diffuse and elongated emission, is interesting for comparing this system with black holes, showing that jets can be produced despite the shallower gravitational potential of NSs (Fender et al. 2004). The orientation of the radio jets has been reported to change with time either because of the precession of the regions from which they are emitted, where it is well accepted that they must be close to the compact object, or because of the interaction with the interstellar matter (Coriat et al. 2019).

Several models have been proposed to account for the peculiar orbital and state variations of Cir X-1. A dip in the light curve—followed by a flaring phase—is seen every orbit. This dip could be caused by a cold absorber; however, this would work only for high inclinations (D'Aì et al. 2012). According to Johnston et al. (1999), the eccentric orbit causes orbital variations in the mass accretion rate, producing the modulation in the X-ray luminosity. Schulz et al. (2019) suggested that the companion is a massive supergiant of Be type, which would imply that Cir X-1 is a high-mass Be XRB. The available observations until now have not been sufficient to discriminate among the different models.

[53] Deceased.

Table 1
Observational Data Used in This Paper, Reporting for Each Mission the Observation IDs, Live Time, and Start and End Times of Each Observation

Mission	ObsID	Live Time (s)	Start Time	End Time
IXPE	2002699	263,000	2023-08-02T11:24	2023-08-04T23:52
			2023-08-11T10:17	2023-08-13T22:46
NICER	6689030104	305	2023-08-05T00:22	2023-08-05T00:35
	6689030203	4325	2023-08-13T00:27	2023-08-13T20:57
NuSTAR	30902037002	12,000	2023-08-04T21:51	2023-08-05T09:01
	30902037004	15,000	2023-08-12T14:31	2023-08-13T01:26

We report the first polarimetric study of Cir X-1 using the Imaging X-ray Polarimetry Explorer (IXPE), measuring the new observables of polarization degree (PD) and polarization angle (PA). With X-ray polarimetry we can discern, from different polarization signatures, the different emission mechanisms and the geometry of the regions closer to the compact object. In the absence of relativistic effects, the PA is expected to be either parallel or perpendicular to the main geometrical axis of the component; as a consequence, if two components (such as a disk and Comptonized region) are aligned, we expect their PAs to be either the same or orthogonal. If this is not the case, it can indicate that there is a geometrical misalignment between them, or that relativistic effects rotate the polarization plane (e.g., Connors & Stark 1977; Connors et al. 1980; Dovčiak et al. 2004; Loktev et al. 2020, 2022).

2. Observations

2.1. IXPE

IXPE (Soffitta et al. 2021; Weisskopf et al. 2022) is the first observatory combining detectors sensitive to X-ray polarization in the 2–8 keV energy band with X-ray optics. This mission, a collaboration between NASA and the Italian Space Agency, consists of three X-ray polarization sensitive gas pixel detectors (Costa et al. 2001; Bellazzini et al. 2006, 2007; Baldini et al. 2021) at the focus of three grazing incidence optics. Other than detecting polarization, IXPE simultaneously detects the energy, time of arrival, and celestial position of each X-ray detected.

IXPE observed Cir X-1 in two different pointings (2023-08-02T11:24 to 2023-08-04T23:52 and 2023-08-11T10:17 to 2023-08-13T22:46, joint in ObsID 02002699; see Table 1) to cover two different parts of the orbit for a net total exposure time of 263 ks. Neutron Star Interior Composition Explorer (NICER) and Nuclear Spectroscopic Telescope Array (NuSTAR) observations were performed to simultaneously partially cover the IXPE observation. IXPE data are reduced and corrected by the standard pipeline running at the Science Operations Center in NASA/MSFC and were downloaded from the IXPE public archive at HEASARC.[54] In the following analysis, event-by-event Stokes parameters are calculated following an unweighted approach (Kislat et al. 2015; Di Marco et al. 2022a) and computed using IXPEOBSSSIM 30.6.3 (Baldini et al. 2022); they are provided to the user in a reference frame projected on the sky. We selected the source in a circular region of radius 90″ centered on the source. Because of the high brightness of this source, the background is negligible (see Di Marco et al. 2023a).

The top panel of Figure 1 shows the IXPE light curve during these observations overlaid with data from the Monitor of All-sky X-ray Image (MAXI; Matsuoka et al. 2009) telescope. MAXI is mounted on board the International Space Station and monitors X-ray sources continuously; therefore, its light curve allows one to study the flux variations in Cir X-1 over its entire orbit, even outside the IXPE observation.

To verify possible changes in the accretion flow of Cir X-1, we study its flux and hardness ratio (HR) variations over the IXPE observing time. The bottom panel of Figure 1 shows the IXPE HR, defined as

$$\mathrm{HR_{IXPE}} = \frac{\text{Counts [4–8 keV]}}{\text{Counts [3–4 keV]}}. \quad (1)$$

The same plots show a division of the overall observations in three phase intervals, which we will use in the following to study the polarization along the orbit of Cir X-1: P1 (phase from 0.21 to 0.22), P2 (phase from 0.22 to 0.36), and P3 (phase from 0.75 to 0.90). We clearly see during the first observation a transition from a low-flux hard state to a high-flux soft state. The IXPE observation starts just when the source is coming out from the dip, as shown by the MAXI light curve, so that the low–hard state corresponds to this part of the orbit.

Figure 2 (left) shows the hardness–intensity diagram for the three phase intervals obtained from the IXPE data. We clearly see a variation in hardness–intensity between the low–hard and high–soft states when moving from the first to the second phase interval. We also see that the HR is, on average, slightly larger in the third phase interval, when the flux is lower, compared to the second phase interval. The same effect is also seen in the color–color diagram (right panel of Figure 2), which shows the evolution of the source in two colors defined for the low- and high-energy bands.

Tominaga et al. (2023) studied Cir X-1 for an extended period and divided (Figure 2 of their paper) the orbit into different phases: a dip phase, where the X-ray flux is low due to strong absorption and whose end corresponds to P1 in this paper; a flaring phase, with rapid changes, corresponding to P2 in this paper; and a stable phase, with a gradual decrease in X-ray flux, corresponding to P3 in this paper.

2.2. NICER

NICER (Gendreau et al. 2016), mounted on board the International Space Station, observed Cir X-1 during part of the IXPE observations. ObsIDs 6689030104 (right at the end of the first IXPE observation) and 6689030203 (during the second IXPE observation; see Table 1) were used to study the spectral components of Cir X-1 (see Section 3). NICER consists of 56 coaligned concentrator X-ray optics, each with a silicon drift detector at its focus, and, although it does not have imaging capabilities, it has a large collecting area in the energy interval of 0.2–12 keV. These observations were obtained in the

[54] https://heasarc.gsfc.nasa.gov/docs/ixpe/archive/

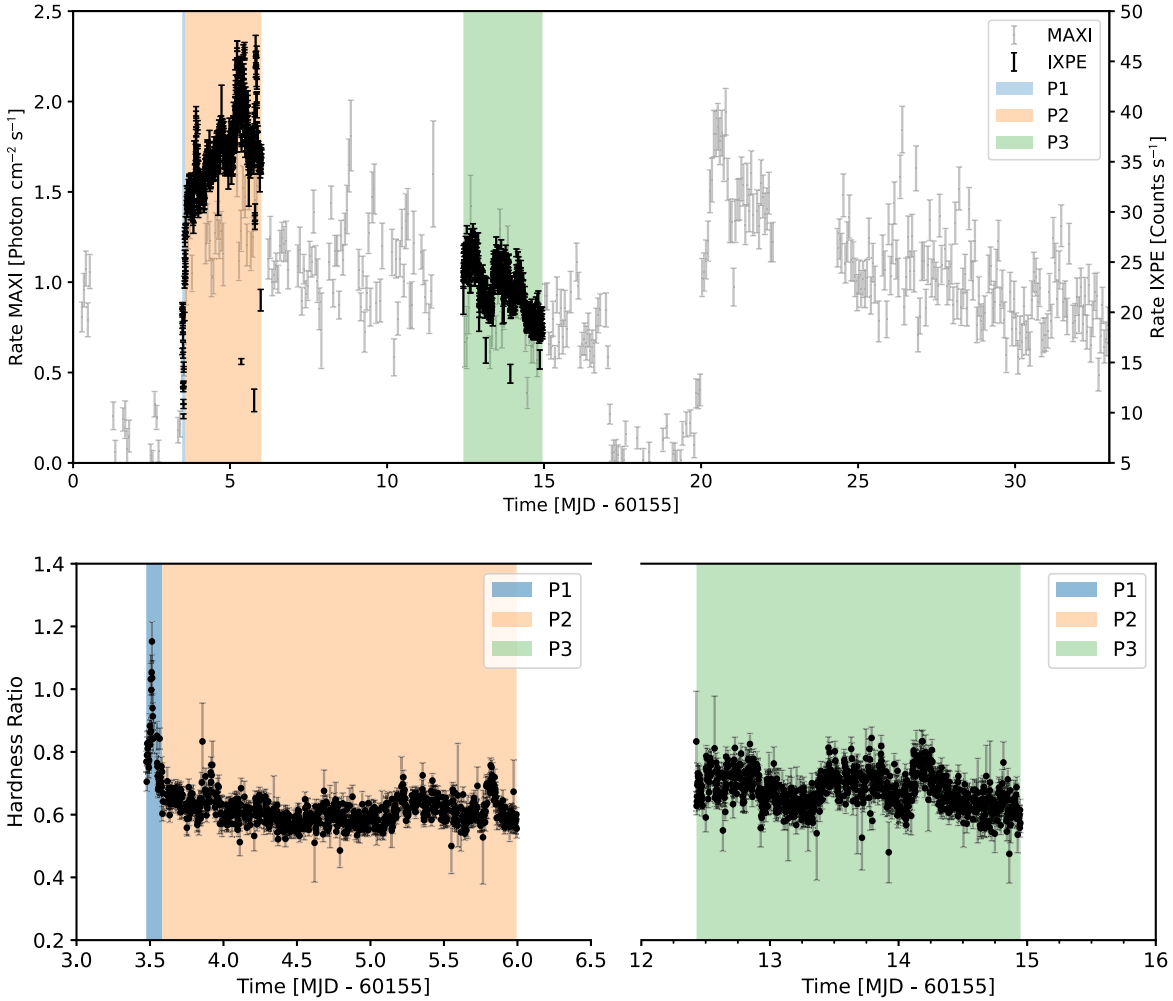

Figure 1. Evolution of the X-ray properties of Cir X-1. (Top) Rate obtained by MAXI (2–20 keV) and IXPE over two orbits binned in 180 s time bins. (Bottom) HR obtained from IXPE (Equation (1)) during the observations binned in 500 s time bins. There is a clear change in state from the hard to the soft at the beginning of the IXPE observation; based on this, we divide the analysis into the three phase intervals indicated in the plots by the colored regions.

framework of GO Cycle 5 (proposal 6189); data were processed with the NICER Data Analysis Software v010a released on 2022 December 16 provided under HEASOFT v 6.31.1 with the CALDB version released on 2022 October 30.

2.3. *NuSTAR*

NuSTAR (Harrison et al. 2013) consists of two focal plane modules (FPMA and FPMB) providing broadband X-ray imaging, spectroscopy, and timing in the energy range of 3–79 keV with an angular resolution of 18″ (FWHM) and spectral resolution of 400 eV (FWHM) at 10 keV, and it is the only observatory employing multilayer X-ray optics capable of focusing hard X-rays. We used the Cir X-1 observations at the end of the first IXPE observation (ObsID 30902037002) and during the second one (ObsID 30902037004; see Table 1), performed in the framework of GO Cycle 9 (proposal 9212).

NuSTAR data were processed using the standard Data Analysis Software (NUSTARDAS v2.1.2 from 2022 February 12) provided under HEASOFT v 6.31.1 with the CALDB version released on 2023 April 4. The source was selected from a circular 150″ radius region centered on the source position; the background was extracted in a similar region but in a position of the field of view out of the source.

3. Spectroscopic Analysis

Aiming to constrain the spectral model and understand the different components, we analyzed NICER (in 1–10 keV) and NuSTAR (in 3–25 keV) data; the ObsIDs are those reported above and were selected to overlap and have a short duration, so that there would be no HR variations. Previous spectral fits, such as in the broadband BeppoSAX spectra (Iaria et al. 2002, 2005), reported the presence of two components: a blackbody disk and a Comptonization component. However, the temperature of one of the components—the disk—has been reported to be low (∼0.5 keV; Iaria et al. 2008), so the disk is not expected to contribute significantly to the IXPE energy band.

We attempted to fit the continuum with the two components reported in the literature: `diskbb` (Mitsuda et al. 1984; Makishima et al. 1986), associated with the disk or NS surface, and `comptt` (Titarchuk 1994), associated with the Comptonization in the BL/SL. We saw an excess in the residuals around 6 keV, associated with a broad iron line due to reflection from the disk, and around 1.7 keV, associated with a silicon line, suspected to be an instrumental NICER feature due to an incorrect calibration of the response, which becomes visible at the high flux observed from Cir X-1. To estimate the absorption from the interstellar medium, we set the abundances